



HAL
open science

Compression of 2-D biomedical images

Christine Cavaro-Menard, Amine Naït-Ali, Olivier Déforages, Marie Babel

► **To cite this version:**

Christine Cavaro-Menard, Amine Naït-Ali, Olivier Déforages, Marie Babel. Compression of 2-D biomedical images. Compression of Biomedical Images and Signals, ISTE-Wiley, pp.155-186, 2008, Digital Signal Processing. hal-00278779

HAL Id: hal-00278779

<https://hal.science/hal-00278779>

Submitted on 14 May 2008

HAL is a multi-disciplinary open access archive for the deposit and dissemination of scientific research documents, whether they are published or not. The documents may come from teaching and research institutions in France or abroad, or from public or private research centers.

L'archive ouverte pluridisciplinaire **HAL**, est destinée au dépôt et à la diffusion de documents scientifiques de niveau recherche, publiés ou non, émanant des établissements d'enseignement et de recherche français ou étrangers, des laboratoires publics ou privés.

Chapter 7

Compression of 2-D Biomedical Images

7.1. Introduction

On a daily basis, large amounts of medical images are acquired using 2D acquisition imaging systems (e.g., vertebra and lung digital X rays, mammography). Moreover, it is possible to compress temporal sequences (i.e. 2D+t), volume sequences (i.e. 3D) or even spatio-temporal sequences (i.e. 3D+t) by encoding each image separately and independently of all others (i.e. in clinical routine, physicians do not always keep all images but instead select the most relevant and accurate ones). Thus, 2D compression is widely applied to medical images. It is also included in the DICOM format (described in Chapter 4), within various PACS.

This chapter is a review of some basic 2D compression methods which are frequently applied to medical images. Although, the common compression techniques and the traditional standards of compression do apply to medical images, some specific methods applied to specific images have been specially developed in order to optimize both the compression rates and the quality of the re-constructed image.

This chapter is made up of three main parts. Section 7.2 will look at the compression of medical images using reversible methods (i.e. lossless). This will be followed by an examination of lossy techniques in section 7.3, and finally, progressive compression methods will be described in section 7.4. Thus, we will show that this type of compression is highly appropriate to the transmission of medical information.

Chapter written by Christine CAVARO-MÉNARD, Amine NAIT-ALI, Olivier DEFORGES and Marie BABEL.

7.2. Reversible compression of medical images

As is well known, reversible compression methods produce an exact duplicate of the original image and are often incorporated by constructors within some acquisition systems. In the medical field, the lossless nature of these methods is of paramount importance for ethical reasons.

The general scheme of reversible compression methods occurs in two stages: a transformation in order to reduce the inter-pixel correlation, and an entropic coding (e.g. Huffman or arithmetic encoder). The transformation must result in integer values for the encoder to function. It can be a transformation by block, by filter banks or a predictive transformation.

7.2.1. Lossless compression by standard methods

A 1998 study [KIV 98] has drawn a detailed comparison of different reversible compression methods using a medical image database made up of 3,000 images from 125 patients. In this study, 10 different gathering techniques have been used: X-ray (lungs), CT (abdomen and head), MRI (abdomen and spine), SPECT (head, heart and total body) and ultrasound. The methods that were tested are the following:

- general compression software such as GZIP, PKZIP, JAR, RAR, YAC, etc.;
- specific methods for the compression of monochrome images:
 - methods that are based on the coding algorithm LZW (derived from the inventors' names Lempel, Ziv and Welch), the PNG standard (*Portable Network Graphics*) and GIF standard (*Graphics Interchange Format*),
 - a method based on a contextual model and RICE coding: the FELICS algorithm (*Fast, Efficient, Lossless Image Compression System*) [HOW 93],
 - methods based on predictive encoding with a fixed predictor: the LJPEG standard (*Lossless JPEG*), the CLIC algorithm (*Context-based Lossless Image Compression*) [TIS 93],
 - methods based on adaptive predictive encoding: the LOCO-I standard (*Low Complexity Lossless Compression for Images*) also known as JPEG-LS [WEI 00], the CALIC algorithm (*Context-based Adaptive Lossless Image Compression*) [WU 97], and the TMW algorithm (a reference derived once again from the authors' names) [MEY 97],
 - methods based on hierarchical predictive encoding: the CPM algorithm (*Central Prediction Method*) [HUA 91], and the BTPC algorithm (*Binary Tree Predictive Coding*) [ROB 97],

- methods based on integer-to-integer wavelet transform (S transform): the SPIHT algorithm (*Set Partitioning in Hierarchical Trees*) [SAI 96a].

To conclude, Kivijärvi *et al.* have suggested that the BTCP and GIF standards are not well-suited to medical images because they only apply to images encoded on 8 bits and because compression rates are directly related to the image type. The best compression rates are obtained by methods specific to images and in particular, using the CALIC algorithm for most of the images, TMW for CT (average compression rates lying between 2.7:1 and 3.8:1), SPIHT for MRI (between 2:1 and 3:1) and JPEG-LS for SPECT (between 2.7:1 and 5:1). Overall, when it comes to medical imaging, the compression rates achieved using reversible compression techniques vary between 2:1 and 5:1. In some cases, they can reach the compression rate 10:1 on specific images that represent large homogenous areas. In terms of execution time, the TMW method was found to be rather time consuming and the JPEG-LS method (lasting about 0.2 to 14 seconds per image) is faster than the CALIC method (lasting between 0.3 and 60 seconds per image) and the SPIHT method (between 0.4 and 90 seconds per image). Of course the execution time depends on the calculation platform.

Similar conclusions have been reached by Adamson following his study on various cerebral CT [ADA 02].

Recently, Clunie [CLU 06] has evaluated the latest versions of the JPEG-LS standard (ISO/IEC 14495-1) (this version links the RLE encoding to the LOCO-I standard) and the lossless mode of JPEG2000 (ISO/IEC CD15444-1) (using the integer-to-integer 5.3 wavelet transform) which may be incorporated within the DICOM, on 3,679 images of different organs and obtained using different gathering techniques. The average compression rates obtained for these methods are similar and of the order of 3.8:1. Depending on the gathering technique, JPEG-LS gives on average the following compression rates: 4:1 for CT images, 3.6:1 for MRI images, 6:1 for SPECT and 3.4:1 for ultrasound.

7.2.2. Specific methods of lossless compression

In order to optimize the compression rates it is possible to make use of the similitude between two T1-weighted MRIs of the abdomen and two CTs of the thorax. The method defined hereafter will be advantageous for the type of image given: the same modality, acquisition parameters, organ and using similar acquisition systems. For predictive encoding methods it is possible to proceed as follows:

- define specific fixed predictors adapted either by adaptable algorithm LMS (Least Mean Square) [NIJ 96] or by pseudo-linear recursive regression [CHE 99];

– define for a given predictor, a statistical model of the prediction error on different regions of the image (such as the image background and the studied area). Thus, a specific codebook will be associated with each region of the image during the statistical encoding [MID 99].

7.2.3. Compression based on the region of interest

Each region of the image may have more or less importance in the diagnostic process. For example, a brain slice can be separated into two distinct regions: the brain area that is useful to establish a medical diagnosis and the image background which provides no useful information. In order to improve the global compression rates of the image, methods based on regions of interest coding (*ROI coding*) adjust the encoding accuracy to fit the diagnosis information present in the image (i.e. the data in ROI is subject to reversible encoding while other areas are coded using lossy techniques). Regions of interest are either defined manually or after segmentation.

Halpern *et al.* have manually depicted the ROI of 75 CT images of the abdomen [HAL 90]. The data present in the ROI is encoded by a quad-tree reversible process and external data is subject to lossy compression method at different compression rates. Whatever the compression rate (i.e. lower than 50:1) applied on the outside of the ROI, the sensitivity (as defined in Chapter 5) is almost always satisfactory (over 90%) and close to that obtained by reversible compression (96%). On this type of image, compression based on ROI allows us to reach compression rates of up to 28:1, (with a maximum compression rate outside the ROI) when the average compression rate for most reversible compression processes is of 3:1.

The latest JPEG2000 version allows a manual determination of various ROI of circular shape and allows us to perform a reversible compression of data contained within the ROI (Chapter 2).

The different regions to be coded can be defined after a segmentation phase. Then the coding strategy for each region can be adapted to the content of the information included in this type of region. This coding method works by separating the image into two parts (its contours and its texture) and represents an image symbolically in the form of a mosaic of adjacent regions with continuous variations in their internal pixel amplitudes. The borders of the regions represent the image's contours and can be coded by a reversible process known as the Freeman differential coding method or by a lossy process which consists of approximating its borders by straight lines for example. The luminance signal in each region corresponds to the texture of each object within the image and can be encoded using various methods with compression rates the levels of which vary according to the information contained in that object.

In medical imaging, a reversible compression of images that hold fine diagnosis information is required. Improving the global compression rate of the image can then be obtained without coding the image's background [CAV 96] (Figure 7.1).

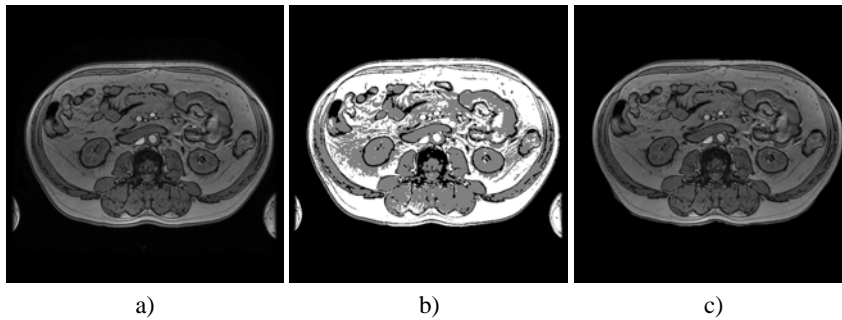


Figure 7.1. a) Original abdominal MRI (512x512x16 bits); b) fuzzy classification into 3 sets based on pixel intensity (the background set of the image in black holding 56% of pixels); c) reconstructed image after a predictive reversible compression of the pixels in all the other sets TC=7.4

Adaptive or optimal predictive encoding on each region to be coded can be performed according to a specific exploration adapted to any kind of region's shape (Figure 7.2).

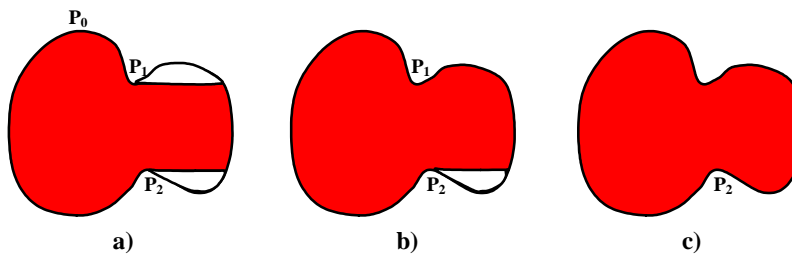


Figure 7.2. Exploration of a region with a shape: a) exploration from top to bottom starting at point P_0 ; b) exploration from bottom to top starting at P_1 ; c) exploration from top to bottom starting at P_2 ; from [CAV 96]

The benefits in terms of compression rate largely depend on the image being studied (i.e. the amount of non-coded data), but according to [CAV 96], coding methods based on the contour-texture approach resulted in improvements of 10 to 30% in compression rates. Such methods are truly promising and can be further improved by re-adapting the process to new diagnostic signal models.

Nevertheless, when a storage process is required, it is impossible to determine which details will be useful in the future [KIV 98]. An initially unimportant detail during the acquisition process may become of great informative value for a pathologic follow-up to determine when a certain disease first appeared. Moreover, many pathologies can spread out over the entire image studied and a single detail during the acquisition process may be an important element to take into consideration for the diagnosis or the treatment.

7.2.4. Conclusion

As we have seen in the above section, strictly reversible systems have limited efficiency in terms of compression rates and do not provide a long-term solution to increasingly important storage and transmission problems. Lossy compression techniques are thus the only solution which allows high compression rates.

7.3. Lossy compression of medical images

Although reversible compression of medical images provides physicians with resulting images of high analytical quality, the compression rates obtained through these methods are low in comparison with the compression rates obtained using irreversible methods, also known as lossy compression methods. As mentioned in Chapter 1, mindsets have changed over the last few years, and physicians, now generally agree, under certain conditions (presented in Chapters 1 and 5), to analyze compressed images using lossy compression methods. This new move towards accepting lossy compression methods is becoming increasingly widespread thanks to the numerous publications now available in this field.

In this section, we will introduce different standard compression methods, i.e., quantization, DCT-based compression, JPEG 2000 compression, fractal compression, and finally some specific compression methods applied to medical images, respectively in sections, 7.3.1, 7.3.2, 7.3.3, 7.3.4 and 7.3.5.

7.3.1. Quantization of medical images

As pointed out in Chapter 2, there are two main forms of quantization: scalar quantization often used at the end of an encoding scheme, and vector quantization (VQ). These methods are described in further detail in [BAR 02], Chapter 2. This section will only address vector quantization, a method which might be appropriate to some specific types of images including medical images.

7.3.1.1. Principles of vector quantization

Vector quantization is a lossy compression technique which consists of allocating a code from a specific dictionary to each block or pixel vector constituting the original image. Using this technique, a given block in the image is compared to a set of dictionary codes. Consequently, the code chosen will be that which minimizes a distance with respect to the original block of the image to be coded. As a result, the image can be stored or transmitted very simply by storing and transmitting the index of each code. To reconstruct an image, the decoder uses the indices from which it extracts the appropriate dictionary codes (Figure 7.3). It seems obvious that the performances of this method depend on the number of codes contained in the dictionary. On the other hand, the complexity in terms of code-search could be increased significantly.

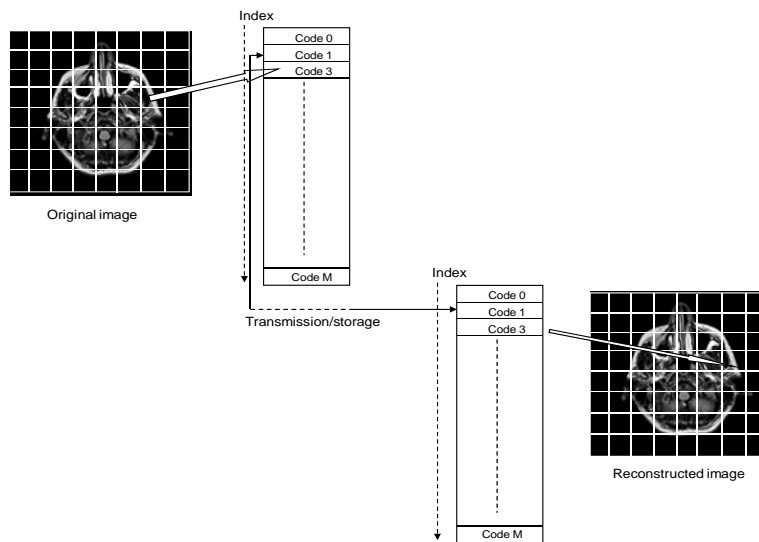


Figure 7.3. Vector quantification scheme

7.3.1.2. A few illustrations

Figure 7.4 shows various results obtained from a vector quantization of a brain MRI image, having a size of 256x256 (Figure 7.4a). Each pixel in this image is coded on 8 bits. In this example, three dictionaries have been tested. The vectors used are in fact, 4x4 or 2x2 matrices. Figures 7.4b, 7.4c and 7.4d show images quantized at a fixed rate. Although the results obtained at 0.3 bpp (CR=25:1) are

obviously unacceptable, the coding 2 bpp (CR=4:1), or even 0.75 bpp (CR=10,5:1) offer an acceptable visual quality.

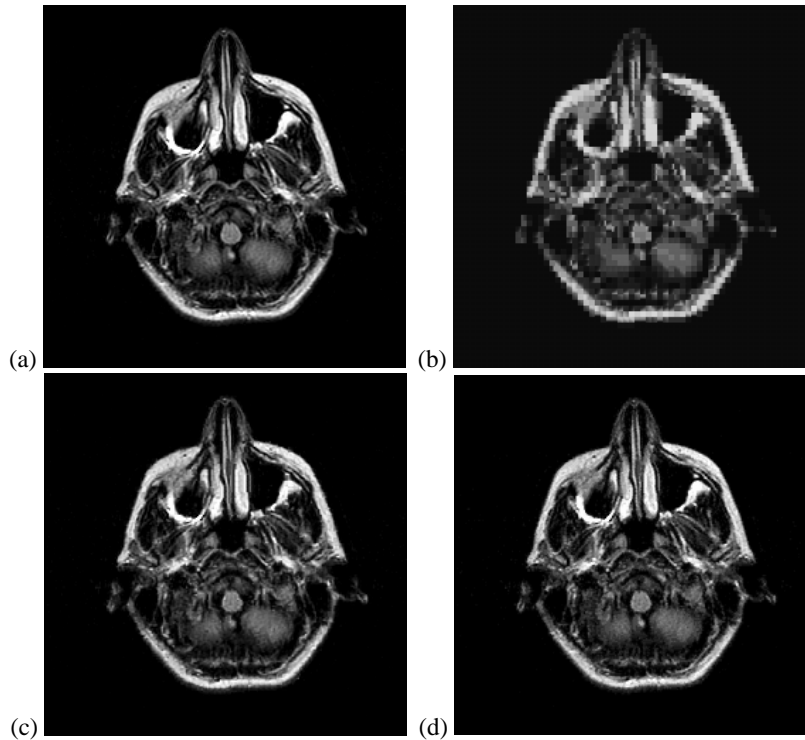


Figure 7.4. Vector quantization applied to a brain MRI:

(a) original image; (b) reconstructed image after vector quantization (2x2), at 0.31 bpp (CR=25:1), PSNR= 24.2 dB; (c) reconstructed image after vector quantization (4x4), at 0.75 bpp (CR= 10,5:1), PSNR= 30.0 dB; (d) reconstructed image after vector quantization (2x2), at 2 bpp (CR= 4:1), PSNR= 33.6 dB

As mentioned previously, one of the disadvantages of the vector quantization is the significant calculation time required for such schemes. More specifically, while searching for a code in the dictionary, the encoder carries out a polling process. Search procedures related to the compression of medical images using rich dictionaries, have often included alternative methods such as the well known tree-structured vector quantization. This can be either balanced or unbalanced.

7.3.1.3. *Balanced tree-structured vector quantization*

As mentioned above, vector quantization involves complex calculations (in order to access codes). This complexity increases in proportion to M , where M stands for the number of codes used in the dictionary. To overcome this problem, tree-structured vector quantization (TSVS) has been developed in [BUS 80] and effectively used in [COS 93] to quantify X-ray and MRI images [RIS 90]. This method enables them to access codes whose complexity increase in proportion to the dictionary size logarithm (Figure 7.5.a).

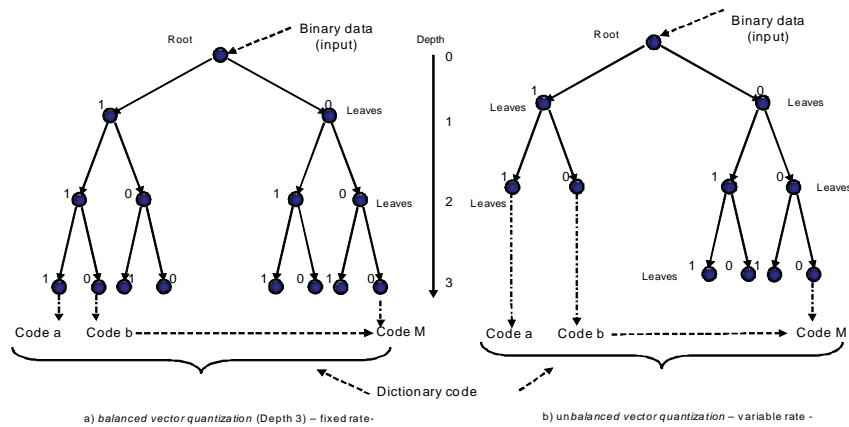


Figure 7.5. Comparison of (a) balanced vector quantization and (b) unbalanced vector quantization

7.3.1.4. *Pruned tree-structured vector quantization*

During vector quantization of medical images, different regions of the image must sometimes be encoded by a higher or lower number of bits, depending on how useful the information is in each of those regions. This is performed by placing the tree-structured leaves at different depths. This method is known as pruned tree-structure vector quantization or PTSVQ (Figure 7.5.b). The PTSVQ always results in variable rates. For more information, the reader can refer to other alternatives, such as EPTSVQ and ECVQ [RIS 90].

7.3.1.5. *Other vector quantization methods applied to medical images*

Table 7.1. shows a set of different approaches applied to medical images and provides a general overview of the different techniques that are developed and evaluated in this context. In this table, the second column indicates the type of medical images used during the evaluation of the given algorithms. The

performances that are recorded in this table will not remain consistent once these techniques are applied to other types of images. In fact, the performance of an encoder is directly related to the specificities of the images being processed.

Methods/approaches	Image Type	Year	Reference
PTSVQ, EPTSVQ, ECVQ	MRI	1990	[RIS 90]
TSVQ	X-Rays	1993	[COS 93]
SVQ	MRI	1996	[MOH 96]
VQ on ROI	Ultrasound	1998	[CZI 98]
DI-VLTSVQ	MRI	1999	[HAN 99]
Quantification by Genetic Algorithms	Ultrasound, X Rays, MRI	2004	[WU 04]

Table 7.1. *Different vector quantization methods applied to medical images*

7.3.2. DCT-based compression of medical images

The consequences of block effect from the JPEG norm on the diagnosis are explained in Chapter 5, section 5.2. This artefact limits the acceptable compression rate in medical imaging to 10:1 [BER 94] [CAV 99].

Based on the DCT transformation of the entire image, Full-Frame DCT compression avoids creating any such artefact. For this reason, it has been widely used in the medical imaging field [CHA 89] [LO 91] [BER 94]. However, it is necessary to adapt the quantization of the DCT coefficients to the specificities of the image being coded. For example, Béretta [BER 94] has segmented the DCT plane into circular frequency zones according to the distribution of frequency components of cardiac angiograms on the DCT plane. The circular zones have been separated according to their direction (horizontal or vertical) (Figure 7.6).

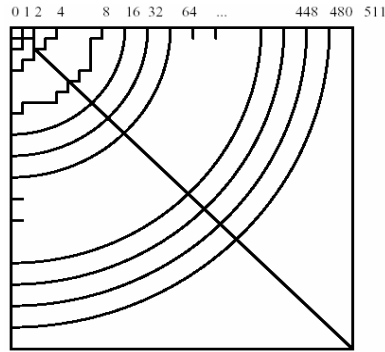


Figure 7.6. Splitting of the DCT map into circular zones with vertical direction (above the diagonal) and horizontal direction (below the diagonal)

Within circular zones, the DCT coefficients generally have low variances. Thus, the same number of bits can be allocated to all coefficients of a circular zone, and the same quantization step can be applied. A truncated Laplacian analytical model can be used to design an optimal midtread uniform quantizer. For an *a priori* number of bits per coefficient and with the observed dynamics and variance of a zone, the optimal quantization step can be calculated, with minimum quantization error. This evaluation can be used in an integer bit allocation algorithm based on the theory of marginal analysis.

On digital cardiac imaging systems, images are enhanced in order to outline the edges of vessels and ventricles. Edge enhancement filters emphasize the visibility of diagnostic information as well as the possible compression artefacts in the image. Therefore, Béretta [BER 95] has suggested incorporating unsharp masking in the DCT domain before performing the quantization (i.e. pre-enhancement) or during the quantization process (i.e. post-enhancement). The table representing the bit allocation will differ if the image edges are enhanced either before or after the quantization process (Figure 7.7).

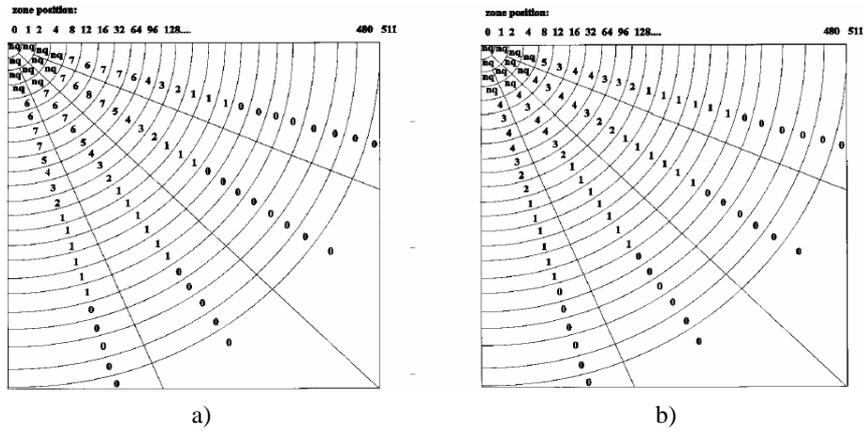


Figure 7.7. a) Bit allocation of the post-enhanced coronary image at $CR=12,6:1$;
 b) bit allocation of the pre-enhanced coronary image at $CR=12,8:1$; from [BER 95]

An inverse filter method has been introduced for calculating a de-enhanced image from the enhanced-compressed one. In fact, images which have not been enhanced are needed for other types of treatments, such as for quantitative measures for example. A regularized restoration can be used to improve the quality of the decompressed de-enhanced image. The results show a significant improvement in the quality of the enhanced image compressed with a Full-Frame DCT transformation, whereas the JPEG coded image shows a blocking effect.

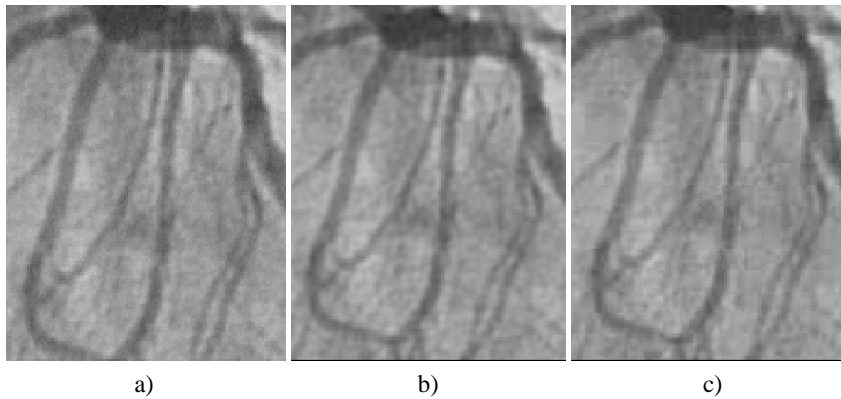


Figure 7.8. a) Original enhanced cardiac angiogram;
 b) pre-enhanced Full-Frame DCT coded image ($CR=12,8:1$);
 c) enhanced JPEG coded image ($CR=12,8:1$); from [BER 95]

7.3.3. JPEG2000 lossy compression of medical images

Recent works have studied the use of JPEG2000 compression on a variety of medical images. Table 7.2 shows the range of acceptable compression rates defined after analyzing the accuracy of the diagnosis. The second section of the fifth chapter outlines the effects of the smoothing effect caused by the JPEG2000.

Image Type	Acceptable compression rate	Reference
Digital chest radiograph	20:1 (so that lesions can still be detected)	[SUN 02], [CAV 01]
Mammography	20:1 (detecting lesions)	[SUR 04]
Lung CT image	10:1 (so that the volume of nodules can still be measured)	[KO 05]
Ultrasound	12:1	[CHE 05]
Coronary angiogram	30:1 (after optimizing JPEG2000 options)	[ZHA 04]

Table 7.2. Applying JPEG2000 compression to different medical images

7.3.3.1. Optimizing the JPEG2000 parameters for the compression of medical images

In this section we will be looking at a compression approach which has been applied to medical images. This technique is based on the optimization of the options of the JPEG2000 standard (Table 7.3) with respect to a given objective function. Zhang *et al.* [ZHA 04] applied this approach to angiograms. In their study, Zhang *et al.* have determined the best set of parameters (JPEG2000 options), which guarantee optimal compression rates while allowing, at the same time, the detection of useful information from the considered image, initially compressed using a lossy technique (Figure 7.9).

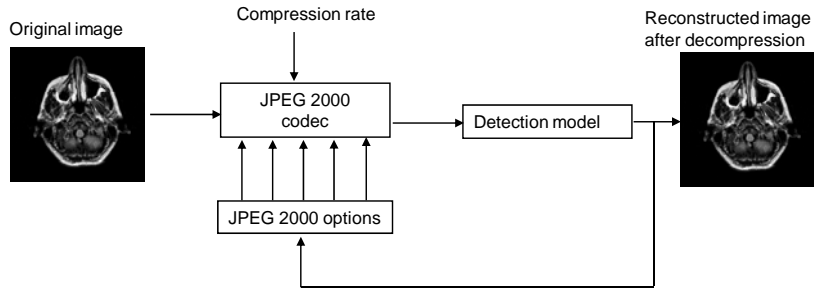


Figure 7.9. Generalized block diagram illustrating the approach proposed in [ZHA 04]

Genes	Coder options	Range
Gene 1	Size: tile	32, 64, [88-92], [108-114], 128, [148-152], [216-240], 256, [436-484], 512 (by default)
Gene 2	Resolution	2, 3, 4, 5, 6 (by default), 7, 8
Gene 3	Mode	Int (by default), real
Gene 4	Size: code-blocks	32x64, 32x32, 64x32, 64x64 (by default), 256x16, 16x256, 16x128, 128x16, 128x32, 32x128, 128x8, 8, 256x8, 8x256
Gene 5	Size: Precinct	256x256, 128x128, 512x256, 64x64, 32x32, 256x512 (by default)

Table 7.3. JPEG2000 options to be optimized

It is important to note that with such an approach, the type of anomaly to be identified, as well as its approximate location within the image, are supposed as being known *a priori* (Figure 7.10).

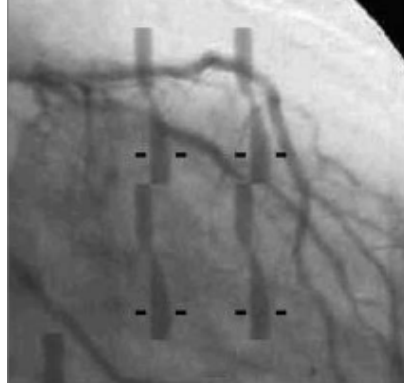


Figure 7.10. Angiogram: the type of anomalies to be detected as well as their location is supposedly already known (between the dark lines, according to [ZHA 04])

The detection model used is known as the NPWE model (*None-Pre-whitening matched filter With an Eye filter*). It is based on the performance of the human visual system, and acts as a meta-heuristic optimizing technique. This model applies genetic algorithms (GA), widely used to minimize (or maximize) non-convex criteria. For further information on how this method works, see [SIA 03]. It is worth noting that the GA uses a stochastic search technique based on the principle of crossover, mutation and reproduction. Figure 7.11 shows a diagram that evaluates the objective function for a fixed *a priori* compression rate.

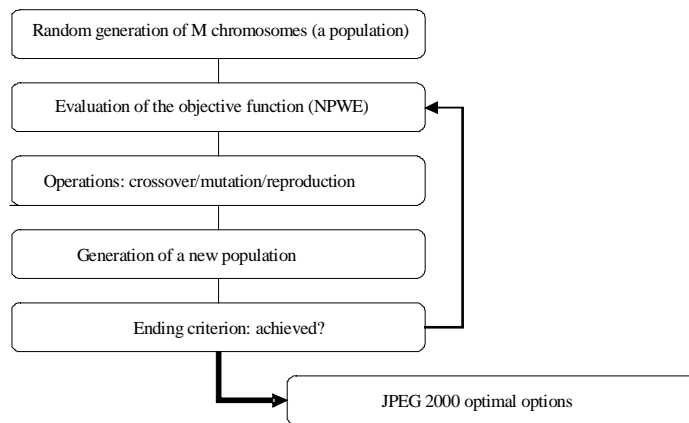


Figure 7.11. Using the GA to optimize JPEG2000 options

This particular algorithm performs iteratively until the appropriate conditions of convergence are reached. Since five different JPEG2000 parameters must be optimized, each chromosome of the GA should include five genes (Figure 7.12).

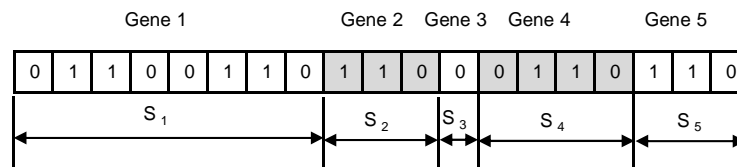


Figure 7.12. Structure of a chromosome used in GA

Although this method is fairly efficient, due to its optimal mode, we must take into consideration the time required by the GA to converge. This process often requires the use of a powerful calculator (e.g. multiprocessor system) to overcome the problem of calculation complexity. Nevertheless, this technique can be used to identify an optimal range of options that fits a given type of image for a given detection model. In other words, a learning phase can be used in order to approximate the optimal values of JPEG 2000 options which can be used *a posteriori* to compress any image of the same type and under the same conditions.

7.3.4. Fractal compression

Fractal compression is widely used on natural images and has been the subject of many publications. However, its use in medical imaging is still rather limited [RIC 98] [KOT 03]. Analyses using ROC curves outlined in these texts clearly show that the quality of the reconstructed image when compressed at a given rate is lower for fractal compressions compared to the results obtained using the DCT-based (e.g. JPEG) method or the wavelet-based one (e.g. JPEG 2000).

The problem of fractal compression can be explained by analyzing the results obtained from cardiac MRIs using the non-optimal FRAP software [RUH 97]. It is clear that the quality of reconstructed images after fractal compression is considerably lower than that obtained using the JPEG2000 standard at rates below 40:1. Beyond this compression rate, the JPEG2000 standard provides low quality images while fractal algorithms are able to maintain a constant image quality even if it is also considered inappropriate for diagnostic purposes. Figure 7.14 illustrates this point.

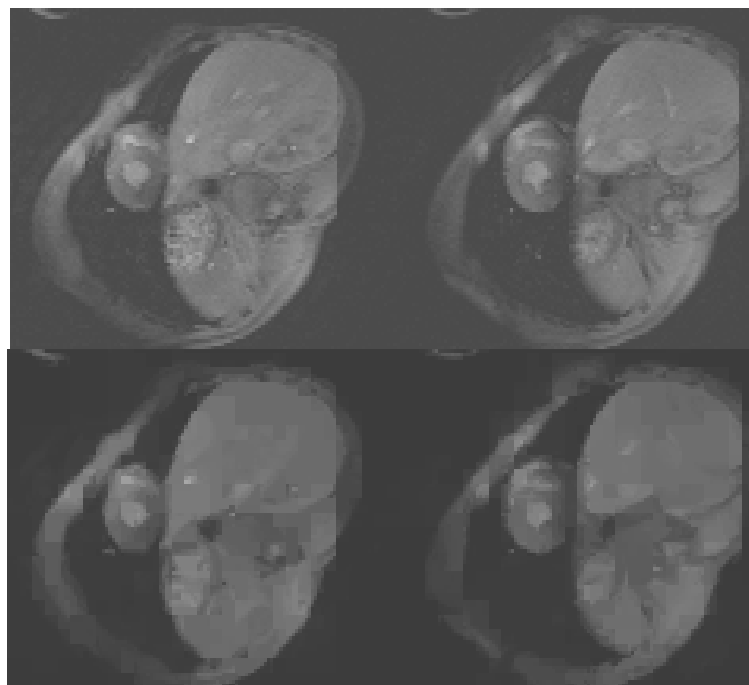


Figure 7.14. *Fractal compression of 2 successive phases on a similar cardiac MRI slice. Above, original images. Below, reconstructed images after fractal compression at a compression rate of 60:1*

7.3.5. Some specific compression methods

7.3.5.1. Compression of mammography images

The encoding method based on regions of interest is widely used for the lossy compression of digital mammography. As an example to illustrate this case, we may refer to the works of Penedo *et al.* [PEN 03], in which they test and compare two techniques with traditional compression methods. One of those techniques is the OB-SPIHT (*Object-Based extension of the Set Partitioning In Hierarchical Trees*) and the other is the OB-SPECK technique (*Object-Based extension of the Set Partitioning Embedded block Coding algorithm*). Since digital mammography is often set against a black background, a segmentation phase is obviously necessary to isolate the tissue from the backdrop as shown in Figure 7.13. The various processing steps following segmentation are:

- encoding of the edges: the edge is often encoded either with or without losses. For further information see [KAN 85] and [EDE 85];
- decomposing the region of interest by wavelets [BAR 94];
- encoding phase using OB-SPIHT or OB-SPECK [SAI 96b], [ISL 99].

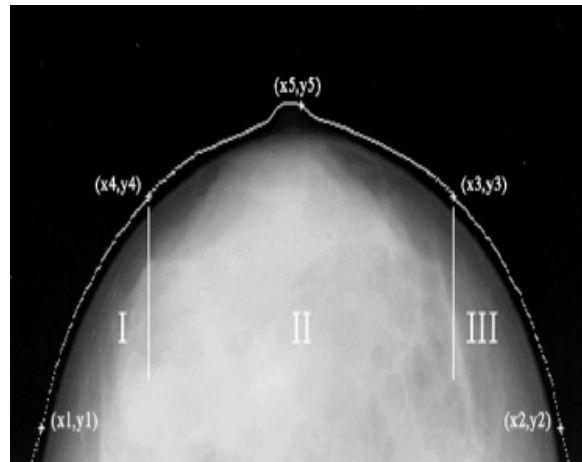


Figure 7.13. Digital mammography in Penedo et al. [PEN 03] (independent encoding of the tissue, edge and background)

7.3.5.2. Compression of ultrasound images

Ideally, it would be best to find a way of combining compression techniques with methods reducing the speckle noise which is specific to ultrasound images. One of the recent works published on this topic deals with ultrasound images through the following distinct steps [GUP 04]:

- calculating the logarithm of the original image (while taking the speckle noise into consideration);
- decomposing the obtained image using wavelets;
- establishing a threshold (after estimation) for the coefficients that correspond to the speckle noise and that are located in different subbands;
- classification of the coefficients organized in subbands in different classes; each class is modelled by a generalized Gaussian;
- carrying out an adaptive quantization of each class;
- carrying out an entropic coding.

For further references see [CHE 05] in which the edges of ultrasound images are restored *a posteriori* by a post-processing technique using morphologic filters.

7.4. Progressive compression of medical images

The design of new encoding techniques is no longer aimed solely at improving performances in terms of compression rates. The development of digital image transmission solutions using different communication media naturally implies new services requiring the adaptation of the coding process to this purpose. Scalable encoding allows the user to download the images progressively; from low quality up to the desired more refined quality. The loading time required for a given image depends on its size, on the transmission rate, on the number of users sharing the same network, etc.

Said has summarized in [SAI 99] the ideal properties of a still image encoding scheme. Among them, we can specifically mention: compression efficiency, scalability, good quality at low bit rates, flexibility and adaptability, rate and quality control, algorithm unicity with/without losses), reduced complexity, error robustness (for instance in a wireless transmission context) and region of interest (ROI) decoding at decoder level.

In the medical imaging context, the use of progressive encoding methods increases network fluidity especially when transmitting over PACS networks or over the Internet. It would be far too ambitious for us to list all the works that have been published in this domain within a single chapter. Nevertheless, section 7.4.1. presents some of the more recent major works relative to this topic. As an example, section 7.4.2 exposes the LAR (*Locally Adaptive Resolution*) progressive compression technique principles. This particular technique has been developed by a French research group.

7.4.1. State-of-the-art progressive medical images compression techniques

As we have seen in Chapter 2, the JPEG2000 standard was specified in such a way that it includes a scalable description of the image. This feature is obtained thanks to on one hand the particular properties of wavelets which allow the decomposition of an image at different resolutions and on the other hand to the use of *codestreams* in order to organise the transmitted information.

Before wavelets were incorporated into the JPEG2000 standard, many researchers were dealing with the problem of progressive compression, defining methods as *lossy to lossless* or even, *lossy to near lossless* compression techniques.

From all the progressive compression solutions that incorporate wavelets, we can cite the one designed by Cristea *et al.* [CRI 98] and applied to MRI images and the one outlined in Munteano *et al.* [MUN 99] and applied to coronary angiograms. These authors propose an approach based on an integer wavelet decomposition scheme (designed through a lifting scheme) and based on intra-band exploration (or non-inter-band) of transformed coefficients. In their respective works, the results have been compared to those obtained by JPEG, SPHIT, and CALIC standards, etc.

In [RAM 06], the SPHIT encoder has been tested on X-ray images, for a progressive transmission on low bit-rate networks. Data is first stored in the DICOM format (Chapter 4). This method involves the modification of the TSUID (*Transfer Syntax Unique Identification*) field inserted in DICOM files header, so as to determine which type of encoder has to be applied on the image. During transmission, the header is first transmitted, followed by the SPHIT compressed image. In this particular study, evaluation is achieved using the following references: JPEG, JPEG-LS and JPEG2000. The authors' conclusions tend to highlight the advantages of the SPHIT compression method; however, the results obtained in this study cannot be generalized to apply to all types of medical images.

In addition to wavelet-based solutions, Grüter *et al.* designed subband decomposition schemes based on non-linear polynomial prediction models [GRU 00]. Evaluations of this particular ROPD (*Rank-Order Polynomial Decomposition*) technique have been performed on MRI, X-ray and ultrasound images. Comparisons have been established using the JPEG methods, SPHIT, WTCQ, etc.

7.4.2. LAR progressive compression of medical images

In this section we describe the LAR method, an encoding technique that tends to fit all the aforementioned characteristics. Section 7.4.2.1 presents the main principles of LAR encoding scheme, as a basis of advanced algorithms. The rest of this presentation deals with the process of encoding medical images only. Section 7.4.2.2 outlines the global progressive scheme and the LAR applications for lossless coding purposes. Section 7.4.2.3 briefly describes the principles of ROI encoding process and its use on medical images. More detailed descriptions, particularly for LAR low bit-rate encoding scheme, are available in [DEF 04] and [BAB 05a].

7.4.2.1. Characteristics of the LAR encoding method

Classically, an image can be described as the superposition of a local texture (fine details) over some low bit-rate global image information (coarse details). The LAR compression method is based on this concept which results in the successful

processing of these two types of data. Thus, the overall scheme of this approach consists of two scalable layers (Figure 7.15): a initial one to encode an image at low bit rates, and a second one for visual quality enhancement at medium/high bit rates.

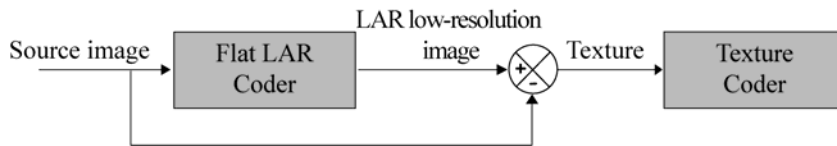


Figure 7.15. General scheme of 2-layer LAR encoding

The first layer of the LAR scheme, named the flat LAR coder, provides a low-resolution image of high visual quality. This image relies on the definition of a specific “quadtree” partitioning process. The size of each block is estimated using a specific criterion measuring local activity, so that smaller blocks are located on the image’s contours, and larger blocks are located in homogenous areas. Figure 7.16 shows the resulting variable-size block representation. The LAR low-resolution image is obtained when filling each block by its mean luminance value. To enhance the visual quality, and taking into consideration the model used to describe block content, a low-complexity post-processing adapted to the variable size-block representation is applied to smooth uniform zones while undamaging contours.

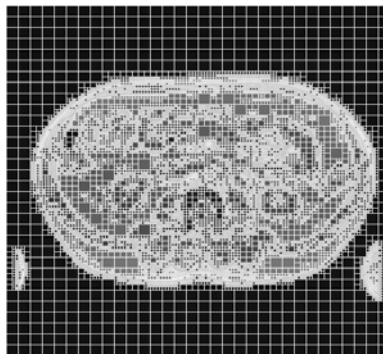


Figure 7.16. Visual representation of the quadtree partitioning proper to the flat LAR coder

The LAR flat coder produces a low bit-rate image. This being so, the main feature of the FLAT coder consists of preserving contours while smoothing homogenous parts of the image. Adapting block sizes to the image content enables high compression ratios together with a satisfactory visual result. Enhancing the low-resolution image is realized using the second layer encoding process (texture

layer). When no quantification is applied, it is thus possible to losslessly encode the image. This feature is particularly relevant when dealing with medical images.

7.4.2.2. Progressive LAR encoding

The scalability concept is particularly relevant in the field of telemedicine; its numerous related uses are indeed naturally useful to most physicians. The simplest version of LAR coding method (two-layer encoding) brings forward an initial notion of scalability. Using an adapted pyramidal decomposition process, the encoding method is transformed into a scalable scheme in terms of distortions and visual quality. The aim is to design a unified coding system able to efficiently address low bit-rates up to lossless compression. For that purpose, three methods have been developed: LAR-APP (Pyramidal LAR approach) [BAB 03], Interleaved S+P [BAB 05b], RWHaT+P (*Reversible Walsh-Hadamard Transform + Prediction*) [DEF 06]. The overall approach used in these three techniques is identical.

To fit the Quadtree partition, dyadic decomposition is carried out. The first and second layers of the flat LAR are replaced by two successive pyramidal descent processes, but the image representation content is preserved: the first decomposition reconstructs the low-resolution image (LAR-image) while the second one processes the local texture information. As shown in Figure 7.17., the first pyramid pass performs a conditional decomposition in accordance with the quadtree partition depicted in Figure 7.16. Consequently the locally content-adapted resolution of the image is successively enhanced, naturally increasing the scalability of the method.

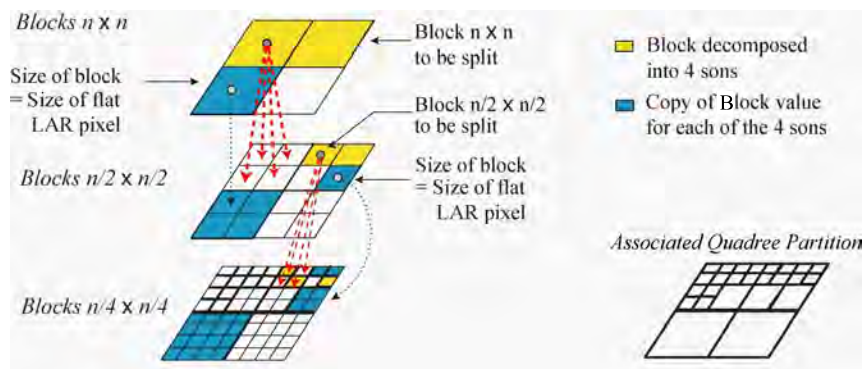


Figure 7.17. Conditional pyramidal decomposition according to the quadtree flat LAR partition

The second pyramidal decomposition, as a dual process, makes it possible to recover the local texture of the image. Blocks that are not decomposed during the first pass are processed during the second one.

As a consequence, pyramidal methods, exploiting the properties of the LAR coding scheme, can be seen as highly scalable methods, in the sense that progressive transmission of data according to resolution or image quality is made feasible. Figure 7.18 shows a typical multi-resolution representation.

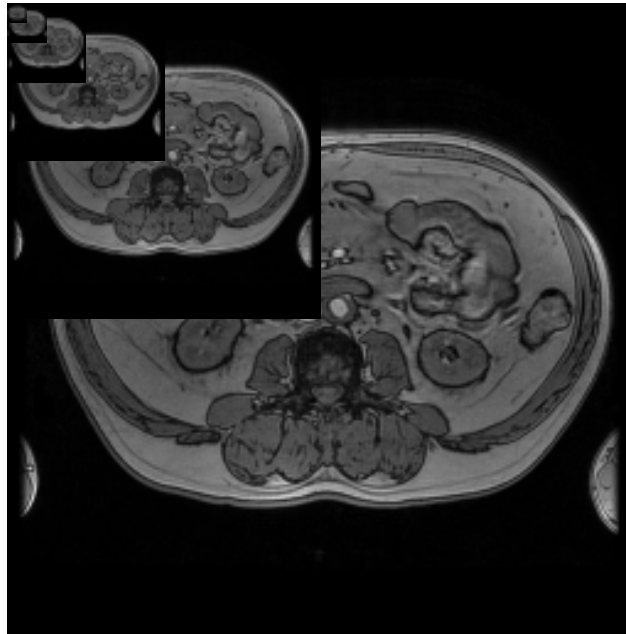


Figure 7.18. *Multi-resolution representation*

Although the three scalable LAR algorithms are based on the same principles, they differ in terms of decomposition stages and pixel encoding processes. The LAR-APP works in the spatial domain using an enriched inter and intra-level prediction. The Interleaved S+P and RWHaT+P methods perform transformation (respectively 1D S-Interleaved transform and 2D Walsh-Hadamard transform) before encoding transformed coefficients using a prediction step.

Performances obtained using the Interleaved S+P method on a large range of medical images are recorded in [BAB 05a]. This particular method largely

outperforms the CALIC method in terms of zeroth-order entropy [WU 95]. Nevertheless, the RWHaT+P algorithm produces better results, in comparison to those obtained by the Interleaved S+P method.

Table 7.4 displays several compression results from the RWHaT+P and Interleaved S+P methods: when compared to CALIC, these results clearly indicate the efficiency of the proposed scheme. Moreover, besides the quantitative aspect of this analysis, the RWHaT+P method offers a scalable solution able to transmit information progressively. Once again this does not apply to the CALIC method.

	Original Entropy (bpp)	Entropy (bpp) CALIC	Entropy (bpp) Interleaved S+P	Entropy (bpp) RWHaT+P
Abdomen1	5.30	3.39	3.11	2.92
MR2DBrain100001	3.55	3.33	2.84	2.76
MR2DBrain100002	3.50	3.30	2.83	2.74
MR2DBrain100003	3.48	3.31	2.83	2.73
MR2DBrain100004	3.53	3.27	2.80	2.69
MR2DBrain100005	3.58	3.29	2.82	2.71
MR2DBrain100006	3.63	3.33	2.88	2.77
XR2DLung1	7.14	2.37	2.45	2.39
XR2DLung2	7.05	2.45	2.51	2.44
XR2DLung3	7.21	2.42	2.49	2.43

Table 7.4. Results of the RWHaT+P and the Interleaved S+P method application on medical images (zeroth-order entropies – bits per pixel)

7.4.2.3. Hierarchical region encoding

Image encoding methods that operate using region representation are highly useful in the sense that they associate both compression and fine descriptions of images. Nevertheless, designing such approaches encounters two recurrent difficulties:

- Shape description, using polygons, produces an information overhead, which can be fairly significant at low bit rates. To reduce this overhead, we need to limit the number of regions to obtain rudimentary simplified regions;
- Region-based methods mainly preserve the “shape” component and often neglect the “content” component. Consequently, for a given representation, an encoded shape becomes independent of its content.

To gradually enhance the quality of reconstructed images while using scalable coding, the idea is to insert a segmentation stage computed at both the coder and the decoder. This stage uses only first-layer rebuilt images and is efficient because the low bit rate LAR images keep their global content, in particular object contours. It leads to a fine hierarchical region representation at no-cost, as no further information is transmitted to describe region shapes.

In fact, the flat layer can be interpreted as a pre-segmentation phase in a split-and-merge segmentation scheme, where small blocks are located on the contours, and larger blocks represent smooth areas. Figure 7.19 illustrates the general LAR region encoding scheme. The choice of resolution level used in the flat LAR coder determines how fine the segmentation will be.

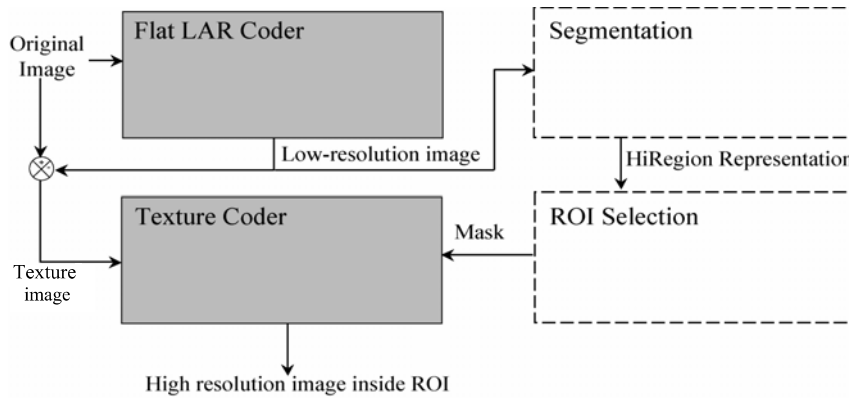


Figure 7.19. General scheme of LAR region encoding

The segmentation algorithm is built upon the intrinsic properties of the LAR low bit-rate image. It involves an iterating, merging process of regions, the initial regions being the blocks from the low-resolution image. Merging is controlled by a single threshold parameter. By iteratively increasing thresholds, a hierarchical segmentation is obtained and enables an efficient description of the image content from finest to coarsest scale. The resulting representation tree can then be scanned globally by level, or locally by region. Figure 7.20. illustrates this type of hierarchical representation obtained at different levels of that tree.

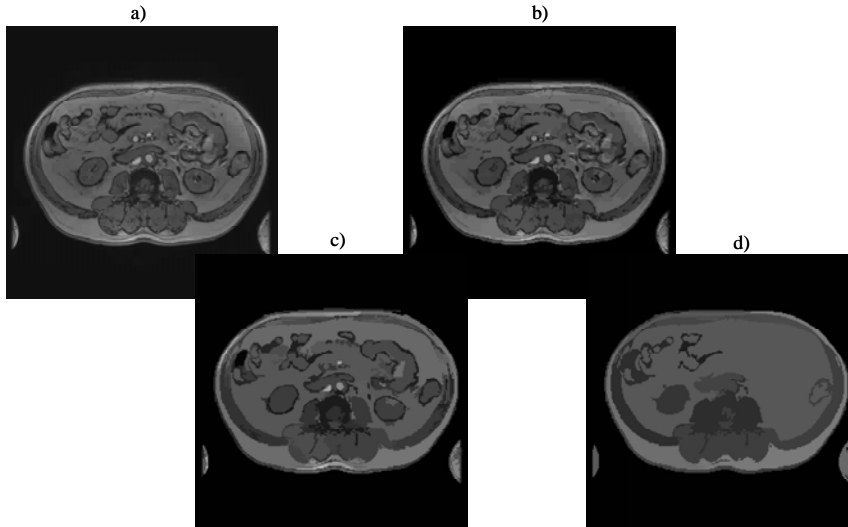


Figure 7.20. Hierarchical region representation from a low bit-rate image of level L1: a) starting level (block representation): 16,202 regions; b) 876 regions; c) 124 regions; d) 18 regions

The main benefit of such a method is that there is immediate, total compatibility between the shape of regions and their coding content. Consequently, one direct application is found in a coding scheme with local enhancement in Regions Of Interest (ROI). From the segmentation map simultaneously available in both coder and decoder, either device can define its own ROI as a set of regions. Thus, an ROI will simply be specified by the labels of its regions.

The method provides a *semi-automatic tool for ROI selection*. Each region, and consequently each ROI, consists of a set of blocks defined in the initial partition. Then *the enhancement of an ROI is straightforward as it merely requires execution of the texture codec for the validated blocks, i.e. those inside the ROI*: the ROI acts simply as a direct on/off control for block-level enhancement. This type of application can easily be implemented using a simple graphic interface that enables us to select the concerned regions. Figure 7.21 illustrates this procedure.

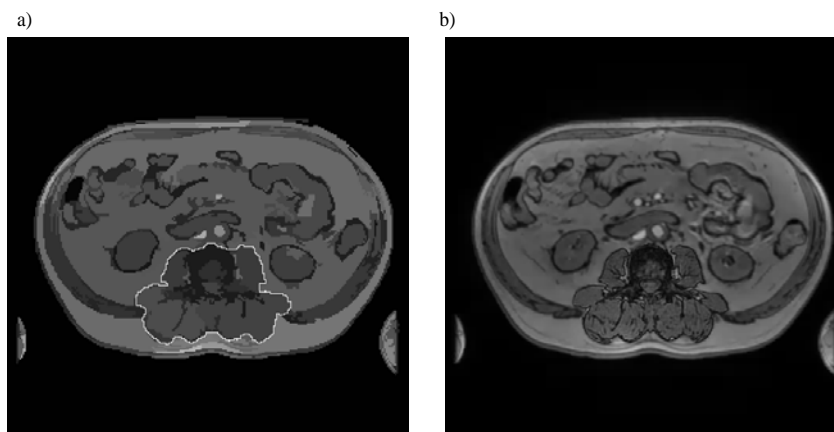


Figure 7.21. ROI encoding: a) 124 regions representation and ROI selection;
 b) low bit-rate encoding of the image background
 (first pass, 0.55 bpp), ROI losslessly coded

7.5. Conclusion

Numerous image compression methods have been developed. They may be defined either as reversible methods (offering low compression ratios but guaranteeing an exact or near-lossless reconstruction of the image), irreversible methods (designed for higher compression ratios at the cost of a quality loss that must be controlled and characterized), or scalable methods (fully adapted to data transmission purposes and enabling lossy to lossless reconstructions). Choosing one method mainly depends on the use of images. In the case of the needs of a first diagnosis, a reversible compression would be most suitable. However, if compressed data has to be stored on low-capacity data supports, an irreversible compression would be necessary. Finally, scalable techniques clearly suit data transmission.

All compression solutions presented in this chapter have been applied, or even adapted for the purposes of medical images. The expression “medical images” represents images of various modalities (X-ray, MRI, ultrasound images, etc.) despite the fact that, as we have seen in Chapter 3, the image specificities and properties differ according to these modalities. As a consequence, the following question remains: why should they all be compressed using the same algorithm? The term “medical image” alone may not and should not justify the use of a particular method. At this stage, we are convinced that it is most pertinent to apply algorithms that are adapted to each type of image. Unsurprisingly, this discussion still remains open.

7.6. Bibliography

- [ADA 02] ADAMSON C., “Lossless compression of magnetic resonance imaging data”, Thesis, Monash University, Melbourne, Australia, 2002.
- [BAB 03] BABEL M., DEFORGES O., ROSIN J. “Lossless and Lossy Minimal Redundancy Pyramidal Decomposition for Scalable Image Compression Technique”, *IEEE ICASSP’03*, Hong Kong, vol. 3, p. 249-252, September 2005.
- [BAB 05a] BABEL M., “Représentation et compression de séquences d’images par la méthode LAR”, PhD Thesis, INSA de Rennes, September 2005.
- [BAB 05b] BABEL M., DEFORGES O., RONSIN J., “Interleaved S+P Pyramidal Decomposition with Refined Prediction Model”, *IEEE ICIP’05*, Gênes, Italy, vol. 2, p. 750-753, September 2005.
- [BAR 94] BARNARD H., “Image and video coding using a wavelet decomposition”, PhD. Dissertation, Dept. Elec. Eng. Delf Univ. Techn., Netherlands, 1994.
- [BAR 02] BARLAUD M., LABIT C., *Compression et codage des images et des vidéos*, Traité IC2, Série traitement du signal et de l’image, Hermes, Paris, 2002.
- [BER 94] BERETTA P., PROST R., AMIEL M., “Optimal bit allocation for Full-Frame DCT coding scheme – Application to cardiac angiography”, *SPIE Image Capture, Formatting and Display*, vol. 2164, p. 291-311, 1994.
- [BER 95] BERETTA P., PROST R., “Unsharp masking and its inverse processing integrated in a compression/decompression scheme – Application to cardiac angiograms”, *SPIE Medical Imaging*, vol. 2431, p. 233-244, 1995.
- [BUS 80] BUZOI A., GRAY A., GRAY R., MARKEL J., “Speech coding based upon vector quantization”, *IEEE Trans. Acous. Speech and Signal Processing*, vol. 28, p. 562-574, 1980.
- [CAV 96] CAVARO-MÉNARD C., “A coding system based on a contour-texture model for medical image compression”, *Innovation et Technologie en Biologie et Médecine*, vol. 17, no. 5, p. 359-371, 1996.
- [CAV 99] CAVARO-MÉNARD C., LE DUFF A., BALZER P., DENIZOT B., MOREL O., JALLET P., LE JEUNE J.J., “Quality assessment of compressed cardiac MRI. Effect of lossy compression on computerized physiological parameters”, *Proceedings of 10th International Conference on Image Analysis and Processing (ICIAP’99)*, Venice, Italy, p. 1034-1037, September 1999.
- [CAV 01] CAVARO-MÉNARD C., GOUPIL F., DENIZOT B., TANGUY J.Y., LE JEUNE J.J., CARON-POITREAU C., “Wavelet compression of numerical chest radiograph: quantitative et qualitative evaluation of degradations”, *Proceedings of International Conference on Visualization, Imaging and Image Processing (VIIP’01)*, Marbella, Spain, p. 406-410, September 2001.
- [CHA 89] CHAN K.K., LOU S.L., HUANG H.K., “Radiological image compression using Full-Frame Cosine transform with adaptive bit-allocation”, *Computerized Medical Imaging and Graphics*, vol. 13, no. 2, p. 153-159, 1989.

- [CHE 99] CHEN Z.D., CHANG R.F., KUO W.J., "Adaptive predictive multiplicative autoregressive model for medical image compression", *IEEE Trans. on Medical Imaging*, vol. 18, no. 2, p. 181-184, 1999.
- [CHE 05] CHEN Y.Y., TAI S.-C., "Enhancing ultrasound by morphology filter and eliminating ringing effect", *European Journal of Radiology*, vol. 53, p. 293-305, 2005.
- [CLU 06] CLUNIE D.A., "Lossless compression of greyscale medical images – Effectiveness of traditional and state of the art approaches", *SPIE MI 2006, Proceedings of SPIE, The International Society for Optical Engineering*, vol. 3980, p. 74-84, 2006.
- [COS 93] COSMAN P., TSENG C., GRAY R., OLSHEN R., MOSES E., DAVIDSON H., BERGIN C AND RISKIN E., "Tree-structured vector quantization of CT chest scans: Image quality and Diagnostic accuracy", *IEEE Trans. on Med. Imag.*, vol. 12, p. 727-739, 1993.
- [CRI 98] CRISTEA P., CORNEALIS J., MUNTEANU A., "Progressive lossless coding medical images", *Future Generation Computer Systems*, vol. 14, p. 23-32, 1998.
- [CZI 98] CZIHO A., CAZUGUEL G., SOLAIMAN B., ROUX C., "Medical image compression using region of interest vector quantization", *Proc. of the 20th Intr. Conf. of the IEEE EMBS*, vol 20, no. 3, 1998
- [DEF 04] DEFORGES O., "Codage d'images par la méthode LAR et méthodologie Adéquation Algorithmique Architecture. De la définition des algorithmes de compression au prototypage rapide sur architectures parallèles hétérogènes", Habilitation à Diriger les Recherches, (HDR), Université de Rennes I, November 2004.
- [DEF 06] DEFORGES O., BABEL M., MOTSCH J., "The RWHT+P for an improved lossless multiresolution coding", *EUSIPCO'06*, Florence, Italy, September 2006.
- [EDE 85] EDEN M., KOCHER M., "On the performance of a contour coding algorithm in the context of image coding. Part I: contour segment coding", *Signal Processing*, vol. 8, p. 381-386, 1985.
- [GUP 04] GUPTA N., SWAMY N., PLOTKIN E., "Despeckling of medical ultrasound images using data and rate adaptive lossy compression", *IEEE Trans. on Med. Imag.*, vol. 24, p. 743-754, 2005.
- [GRU 00] GRÜTER R., EGGER O., VESIN J.M., "Rank-order polynomial subband decomposition for medical image compression", *IEEE Transactions on Medical Imaging*, vol. 19, p. 1044-1052, October 2000.
- [HAL 90] HALPERN E.J., PREMKUMAR A., MULLEN D.J., NG C.C., LEVY H.M., NEWHOUSE J.H., AMIS E.S., SANDERS L.M., MUN I.K., "Application of region of interest definition to quadtree-based compression of CT images", *Invest. Radiology*, vol. 25, no. 6, p. 703-707, June 1990.
- [HOW 93] HOWARD P.G., VITTER J S., "Fast and efficient lossless image compression", *Proceedings of the IEEE Data Compression Conference 1993*, p. 351-361, 1993.
- [HUA 91] HUANG L., BIJAOUI A., "An efficient image compression algorithm without distortion", *Pattern Recognition Letters*, vol. 12, p. 69-72, 1991.

- [ISL 99] ISLAM A., PEARLMAN W., "An embedded and efficient low-complexity hierarchical image coder", *Proc., SPIE*, vol. 3653, p. 294-305, 1999.
- [KAN 85] KANEKO T., OKUDAIRA M., "Encoding of arbitrary curves based on the chain code representation", *IEEE Trans. Comm.*, vol. 33, p. 697-707, 1985.
- [KIV 98] KIVIJÄRVI J., OJALA T., KAUKORANTA T., KUBA A., NYUL L., NEVALAINEN O., "A comparison of lossless compression methods for medical images", *Computerized Medical Imaging and Graphics*, vol. 22, p. 323-339, August 1998.
- [KO 05] KO J.P., CHANG J., BOMSZTYK E., BABB J.S., NAIDICH D.P., RUSINEK H., "Effect of CT image compression on computer-assisted lung nodule volume measurement", *Radiology*, vol. 237, no. 1, p. 83-88, 2005.
- [KOT 03] KOTTER E., ROESNER A., TORSTEN WINTERER J., GHANEM N., EINERT A., JAEGER D., UHRMEISTER P., LANGER M., "Evaluation of lossy data compression of chest X-rays: a receiver operating characteristic study", *Investigative Radiology*, vol. 38, no. 5, p. 243-249, 2003.
- [LO 91] LO S. C., HUANG H. K., "Full-Frame entropy coding for radiological image compression", *SPIE Image Capture, Formatting and Display*, vol. 1444, p. 265-271, 1991.
- [MEY 97] MEYER B., TISCHER P., "TMW a new method for lossless image compression", *Proceedings of International Picture Coding Symposium*, Berlin, p. 217-220, 1997.
- [MID 99] MIDTVIK M., HOVIG I., "Reversible compression of MR images", *IEEE Trans. on Medical Imaging*, vol. 18, no. 9, p. 795-800, 1999.
- [MOH 96] MOHSENIAN N., SHAHRI H., NASRABADI N., "Scalar-vector quantization of medical images", *IEEE Trans. on Image Processing*, vol. 12, p. 727-739, 1993.
- [MUN 99] MUNTEANU A., CORNELIS J., "Wavelet-based lossless compression of coronary angiographic images", *IEEE Transactions on Medical Imaging*, vol. 18, p. 272-281, 1999.
- [HAN 99] HAN J., KIM H., "A differential index assignment scheme for tree-structured vector quantization", *IEEE Trans. on Medical Imaging*, vol. 18, p. 442-447, 1999.
- [NIJ 96] NIJIM Y.W., STEARNS S.D., MIKHAEL W.B., "Differentiation applied to lossless compression of medical images", *IEEE Trans. on Medical Imaging*, vol. 15, no. 4, p. 555-559, 1996.
- [PEN 03] PENEDO M., PEARLMAN W., TAHOSES P., SOUTO M., VIDAL J., "Region-based wavelet coding methods for digital mammography", *IEEE Trans. on Med. Imag.*, vol. 22, no. 10, p. 1288-1296, 2003.
- [PEN 05] PENEDO M., SOUTO M., TAHOSES P.G., CARREIRA J.M., VILLALON J., PORTO G., SEOANE C., VIDAL J.J., BERBAUM K.S., CHAKRABORTY D.P., FAJARDO L.L., "Free-response receiver operating characteristic evaluation of lossy JPEG2000 and object-based set partitioning in hierarchical trees compression of digitized mammograms", *Radiology*, vol. 237, no. 2, p. 450-457, November 2005.

- [RAM 06] RAMAKRISHMAN B., SRIRAAM N., "Internet transmission of DICOM images with effective low bandwidth utilization", *Digital Signal Processing*, vol. 16, no. 6, p. 824-831, 2006
- [RIC 98] RICKE J., MAASS P., LOPEZ HANNINEN E., LIEBIG T., AMTHAUER H., STROSZCZYNSKI C., SCHAUER W., BOSKAMP T., WOLF M. "Wavelet versus JPEG (Joint Photographic Expert Group) and fractal compression. Impact on the detection of low-contrast details in computed radiographs", *Investigative Radiology*, vol. 33, no. 8, p. 456-463, 1998.
- [RIS 90] RISKIN E, LOOKKABAUGH, CHOU P., GRAY R., "Variable rate vector quantization for medical image compression", *IEEE Trans. on Medical Imaging*, vol. 9, p. 290-298, 1990.
- [ROB 97] ROBINSON J.A., "Efficient general-purpose image compression with binary tree predictive coding", *IEEE Transactions on Image Processing*, vol. 6, no. 4, p. 601-608, 1997.
- [RUH 97] RUHL M., HARTENSTEIN H., SAUPE D. "Adaptive partitioning for fractal image compression", *IEEE International Conference on Image Processing ICIP'97*, Santa Barbara, October 1997.
- [SAI 96a] SAID A., PEARLMAN W.A., "Image multi-resolution representation for lossless and lossy compression", *IEEE Transactions on Image Processing*, vol. 5, no. 9, p. 1303-1310, 1996.
- [SAI 96b] SAID A., PEARLMAN W., "A new fast and efficient image codec based on set partitioning in hierarchical trees", *IEEE Trans. Circuits, Syst. Video Techno.*, vol. 6, p. 243-250, 1996.
- [SAI 99] SAID A., "Wavelet-Based Image Compression", Imaging Technology Department, Hewlett Packard Laboratories, 1999.
- [SIA 03] SIARRY P., DRÉO J., PÉTROWSKI A., TAILLARD E., "*Métaheuristiques pour l'optimisation difficile*", Edition Eyrolles, 2003.
- [SUN 02] SUNG M.M., KIM H.J., YOO S.K., CHOI B.W., NAM J.E., KIM H.S., LEE J.H., YOO H.S., "Clinical evaluation of compression ratios using JPEG2000 on computed radiography chest images", *Journal of Digital Imaging*, vol. 15, no. 2, p. 78-83, June 2002.
- [SUR 04] SURYANARAYANAN S., KARELLAS A., VEDANTHAM S., WALDROP S.M., D'ORSI C.J., "A perceptual evaluation of JPEG2000 image compression for digital mammography: contrast-detail characteristics", *Journal of Digital Imaging*, vol. 17, no. 1, p. 64-70, 2004.
- [TIS 93] TISCHER P.E., WORLEY R.T., MAEDER A.J., GOODWIN M., "Context-based lossless image compression", *The Computer Journal*, vol. 36, no. 1, p. 68-77, 1993.
- [WEI 00] WEINBERGER M. J., SEROUSSI G., SAPIRO G., "The LOCO-I lossless image compression algorithm: Principles and standardization into JPEG-LS", *IEEE Transactions on Image processing*, vol. 9, p. 1309-1324, 2000.
- [WU 95] WU X., MEMON N., "A Context-based, Adaptive, Lossless/Nearly-Lossless Coding Scheme for Continuous-Tone Images (CALIC)", International Standards Organization working document, ISO/IEC SC29/WG 1/N256, vol. 202, 1995.

- [WU 97] WU X., MEMON N.D., "Context-based adaptive lossless image compression", *IEEE Transactions on Information Theory*, vol. 23, p. 337-343, 1997.
- [WU 04] WU Y., "GA-based DCT quantisation table design procedure for medical images", *IEEE Proc. Vis. Image Signal Processing*, vol. 151, no. 5, p. 353-359, 2004.
- [ZHA 04] ZHANG Y., PHAM B., ECKSTEIN M., "Automated optimization of JPEG2000 Encoder options based on model observer Performance for detecting variable signals in X-Ray coronary angiograms", *IEEE Trans. on Med. Imag.*, vol. 23, p. 459-474, 2004.